Synthesis of Monodispersed Hollow Silica Nanospheres with Ultrafine Grain Size for Optical Polymer

Xiaofeng Pei[1], Junjie Wang[1], Liangliang Zhang[1], Chao Yang[1], Changwei Cui[1], Xiaofei Zeng[1], and Jianfeng Chen[1]

[1]Beijing University of Chemical Technology

April 16, 2024

Abstract

Hollow silica nanospheres (HSNs) have been widely used as antireflection coatings. However, it is difficult to incorporate them into optical polymer matrices because of their larger size and agglomerations problem, making the haze and transparency worse. Herein, the sub-20 nm HSNs were firstly synthesized by a reverse microemulsion method and the scale-up preparation was successfully achieved in a rotating-packed-bed reactor. The prepared nanocomposites possess super-high transparency and almost unchanged haze.

Synthesis of Monodispersed Hollow Silica Nanospheres with

Ultrafine Grain Size

for Optical Polymer

Xiao-Feng Pei[a,b], Jun-Jie Wang[a,b], Liang-Liang Zhang[b]*, Chao Yang[a,b], Chang-Wei Cui[b], Xiao-Fei Zeng[a,b,]*, Jian-Feng Chen[a,b]

a. State Key Laboratory of Organic-Inorganic Composites,

b. Research Center of the Ministry of Education for High Gravity Engineering and Technology,

Beijing University of Chemical Technology, Beijing 100029, PR China

* Corresponding author:

Xiao-Fei Zeng, Tel: +86-10-64447274; Fax: +86-10-64423474; E-mail:

zengxf@mail.buct.edu.cn

Liang-Liang Zhang, Tel: +86-10-64447274; Fax: +86-10-64423474; E-mail: 2016500003@buct.edu.cn

Significance

Hollow silica nanospheres (HSNs) have been widely used as antireflection coatings. However, it is difficult to incorporate them into optical polymer matrices because of their larger size and agglomerations problem, making the haze and transparency worse. Herein, the sub-20 nm HSNs were firstly synthesized by a reverse microemulsion method and the scale-up preparation was successfully achieved in a rotating-packed-bed reactor. The prepared nanocomposites possess super-high transparency and almost unchanged haze.

Keywords: HSNs, reverse microemulsion, rotating-packed-bed, refractive index, anti-reflection function

Introduction

With the rapid development of nanotechnology, the emergence of hollow nano-materials has impelled the application of nanomaterials into a different fields.[1-5] Among them, HSNs have been widely applied in diverse engineering and technological domain including optical, catalysis and biomedical materials.[6-8] As for the optical materials, HSNs as the anti-reflection agent or coating can effectively reduce the refractive index of materials and enhance their visible transmittance, which have a significant application prospect in the fields of optical transmission, optical storage, and photoelectric display.[9-11]

The main preparation methods of HSNs are templating strategies, which are further divided into three categories as follow: (i) self-template, (ii) soft template, and (iii) hard template.[12-14] Among them, the third method is the most well-defined and has been widely applied in preparation of HSNs.[12] Jia et al.[15] synthesized HSNs by using poly (acrylic acid) as template, ethyl orthosilicate as precursor respectively. As antireflective layer, the average transmittance reached 99% in the wavelength from 380 to1600 nm. Zhang et al.[8] also prepared poly (acrylic acid)-silica core-shell nanospheres and then obtained HSNs by removing core. The particle size of the product is less than 30 nm with obvious hollow structure, which is suitable for anti-reflection coating on solar glass of photovoltaic modules. However, the as-prepared HSNs are usually used as the thin-film coating to enhance the visible transmittance of materials. Incorporation of HSNs into optical polymer matrices to fabricate optical nanocomposites is rarely reported because it is difficult to disperse them well in matrices with the aggregate size less than 40 nm. According to the Rayleigh scattering principle, particles or particles aggregations with the size over 40 nm in optical materials can cause the light scattering.[16, 17] HSNs can theoretically decrease the refractive index of transparent polymer to reduce the surface reflection, whereas they can also increase the light scattering inside the polymer caused by their larger grain size or agglomerations, resulting in that the haze is increased obviously and the total light transmittance may be decreased. So, the synthesis of ultrafine and well-dispersed HSNs is particularly important for the gradient index optical materials.

In this letter, we have firstly synthesized sub-20 nm HSNs by hard template method in water-in-oil system. The prepared HSNs are monodispersed in water and some organic solvents by changing the modifier assortment. The uniformity and output of HSNs can be improved by high-gravity technology in a rotating-packed-bed (RPB). The refractive index of the HSNs is 1.342, which can be well-dispersed in optical polymer matrix to reduce the reflection and therefore boost the transparency remarkably, meanwhile the haze is barely increased.

Experiment Section

In this work, the detailed information regarding all of the reagents, the preparation process for ZnO and HSNs and characterization methods can be found in the Supporting Information.

Results and Discussion

As a template, the prepared ZnO nanoparticles have a spheroid morphology (Fig. 1a) with a narrow size distribution, and the average diameter of nanoparticles is about 9 nm (Fig. 1b), which can be monodispersed in water to form nanodispersion with high transparency (lower left of Fig. S1, Supporting Information). Clear and continuous lattice fringes of ZnO nanoparticles with 0.28 nm lattice spacing in the high resolution transmission electron microscopy image (the lower right inset in Fig. 1a) correspond to the (100) crystal plane of ZnO, which indicates the ZnO nanocrystals are well crystallized.[18]X-ray diffraction (XRD) patterns of ZnO nanoparticles (Fig. 1c) present all the peaks of unmodified and modified samples expectedly corresponding to hexagonal wurtzite crystal form (JCPDS No.361451).[18, 19] All peaks of the modified sample are slightly broadened and weakened than unmodified one, because organic modifier molecules coated on the nanoparticles surface weaken the detection of ZnO crystal components.[18] The FTIR spectrum of ZnO nanoparticles (Fig. 1d) shows that KH550 has been successfully grafted onto the surface of nanoparticles because its characteristic absorption peaks appear in the curve of modified ZnO such as -CH- (2947 cm^{-1}), -CH_2 (1220 cm^{-1}) and -NH_2 (1587 cm^{-1}).[20] Without doubt, KH550-modified ZnO nanoparticles can be well dispersed in the aqueous phase, as shown in Fig. 1a. In addition, the absorption peaks at 3428 cm^{-1} corresponds to the characteristic peaks of -OH stretching vibration. Thermo- gravimetric analysis (TGA)

results furtherly confirm that ZnO nanoparticles were wrapped by the KH550 and the loading is 18.6% (Fig. S1, Supporting Information). It is noted that surface amination treatment makes ZnO nanoparticles positively charged up to 34.2 mv, which facilitates coating process of SiO_2 with negative charge.[21]

HSNs were prepared by the reverse microemulsion method. As shown in Fig. 2a, the microemulsion is composed of water as the disperse phase and cyclohexane as the continuous oil phase, Igepal CO-630 as the emulsifier contributing to the formation of a stable water-in-oil emulsions. ZnO nanoparticles are monodispersed in water nuclear and methyl orthosilicate (TMOS) precursor is dissolved in cyclohexane. Moreover, $NH_3{\cdot}H_2O$ is selected as hydrolysis catalyst, and meanwhile as the etchant for template agent. TMOS in oil phase hydrolyzes at the oil-water interface under the catalytic effect of $NH_3{\cdot}H_2O$ in water and the hydrolysis products enter into water nuclear for heterogeneous nucleation on the surface of ZnO nanoparticles.[22, 23] The amount of water in microemulsion is small, resulting in the achievement of the uniform coating of SiO_2 on ZnO by controlling the hydrolysis reaction rate of TMOS. At the same time, ZnO nanoparticles are corroded slowly and gradually by $NH_3{\cdot}H_2O$ in water. After 2 h reaction, modifier such as polyethylene pyrro-

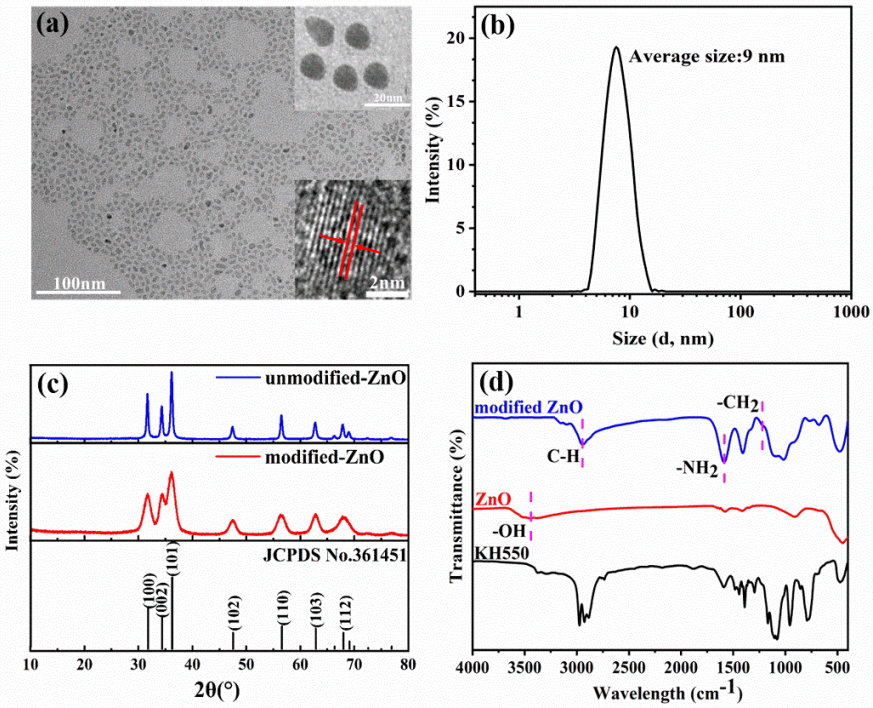

Fig. 1. (a) TEM image and HRTEM image of ZnO nanoparticles (The upper right corner lies the local enlarged view). (b) Particle size distribution of ZnO nanoparticles. (c) FTIR spectra of ZnO nanoparticles. (d) XRD patterns of ZnO nanoparticles.

lidone (PVP) dissolved in water is dropwise added and coated on the surface of SiO_2 by in-situ modification method. After forming a firm SiO_2 coating, the ZnO template disappears and a hollow structure was formed. And thus the modified HSNs are finally obtained. The whole preparation process is performed in RPB, which can produce high gravity environment (tens to hundreds of g) by centrifugal force. The process in the RPB reactor is thus significantly intensified, helpful to providing a more even emulsion system and reaction surrounding, which is suitable for the preparation of uniform nanoparticles at a large-scale.[24, 25]

The effects of different preparation conditions on the morphology and dispersibility of HSNs were investigated and the results show that molar ratio of $NH_3{\cdot}H_2O$ to ZnO is the most critical factor to form an obvious hollow structure in the preparation process. TEM images of SiO_2 nanoparticles prepared in RPB

at different molar ratio of $NH_3{\cdot}H_2O$ to ZnO (Fig. 2b-e) have presented that SiO_2nanoparticles undergo a transition from a solid structure to an inconspicuous hollow structure, then to an obvious hollow structure and final to a core-shell structure with the value decreasing from 7.7 to 3.7. More $NH_3{\cdot}H_2O$ will corrode ZnO rapidly and SiO_2 nucleates independently. Less $NH_3{\cdot}H_2O$ cannot corrode ZnO to form ZnO@SiO_2 nanoparticles with a core-shell structure. Under the optimum ratio of 6.1, the deposition rate matches the corrosion rate of template, and the product can be prepared with high uniformity and well-controlled morphology. In addition, other influence factors such as reaction temperature (Fig. S2, Supporting Information), reaction time (Fig. S3, Supporting Information) and types of modifiers also have important effects on the morphology and dispersion state of HSNs. The results show that 20°C of reaction temperature and 3 h of reaction time are necessary to attain ideal products. With the modification of different kinds of modifiers (PVP, 3-methacryloxypropyltrimethoxysilane, 3-mercaptopropyltrimethoxysilane), HSNs can be stably monodispersed in corresponding solvents (water, methyl isobutyl ketone and MeOH) to form the transparent dispersions.

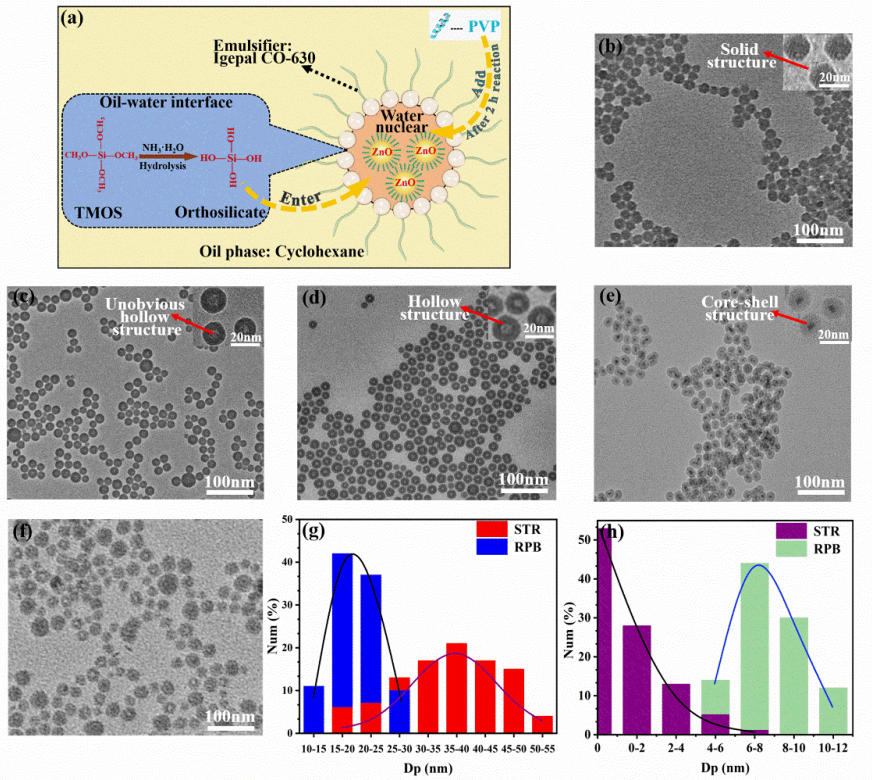

Fig. 2. (a) Reaction mechanism diagram for TMOS in reverse microemulsion. (b-e) TEM of SiO_2 nanoparticles prepared in RPB at different molar ratio of NH3·H_2O to ZnO. (b) 7.7, (c) 6.9, (d) 6.1, (e) 3.7. (f) TEM of SiO_2nanoparticles prepared in STR. (g-h) Histogram of size distribution for SiO_2 nanoparticles prepared in RPB and STR. (g) Particle size distribution. (h) Size distribution of inner cavity.

Processing capacity of RPB reactor for synthesis of such HSNs mentioned above is 1.5 g per batch. The same scale of preparation in STR were studied for comparison. The products are solid and hollow SiO_2 nanoparticles existing simultaneously (Fig. 2f) under the optimum operation conditions in STR, and further prolongation of reaction time in STR would not improve their hollow structure. The particle size distribution of SiO_2nanoparticles and their cavity size synthesized in RPB or STR have been analyzed (Fig. 2g and 2h). The average particle size of SiO_2 nanoparticles is only 19.8 nm with a narrow distribution from 10 to 30 nm for RPB, compared with average particle size of 34.0 nm with a broad distribution from 10 to 50 nm for

STR. Furthermore, the average diameter of inner cavity is about 8 nm for RPB, while it is far less than 8 nm for STR due to more than half of nanoparticles without the hollow structure. More importantly, the reaction time in RPB is 3 h as half as that in STR, resulting from the formation of uniform water-in-oil emulsions with smaller size of water phase and faster mass transfer at oil-water interface in RPB.[25] Moreover, the yields (The mass percentage of the well-dispersed nanoparticles in the total output) of HSNs in RPB and STR with the morphology as shown in Fig. 2d and 2f have a huge difference. The yield in RPB is beyond 70%, which is twice as much as that in STR. All in all, the high gravity technology provides the possibility for the large scale-up preparation of ultrafine HSNs, which is important for the industrial application of HSNs as antireflection functional additive in optical polymer matrices.

From the FT-IR spectra of HSNs (Fig. 3a), it can be seen that unmodified HSNs has no C-H (2969cm^{-1}), C=O (1644cm^{-1}) and C-N (1398cm^{-1}) peaks (characteristic absorption peak for PVP), which appear in the modified ones, indicating PVP are successfully wrapped on HSNs. However, there is no new characteristic absorption peak, illustrating only existence of physical interaction between PVP and HSNs in modified HSNs. Moreover, there are a large number of –OH on the surface of HSNs, resulting in the appearance of -OH stretching vibration peaks at 3384 cm^{-1}. XRD patterns of HSNs (Fig. 3b) exhibits only one wide diffraction peak at about 25deg, indicating that the HSNs present an amorphous state. In the TGA curves of HSNs (Fig. 3c), the weight loss of unmodified and modified HSNs are 5.9 wt% and 21.8 wt % at 800degC respectively. Combined with the results of FT-IR, they are mainly due to elimination of -OH bonds and decomposition of PVP on the surface of nanoparticles respectively, and the coating amount of PVP is about 15.9 wt%.

The refractive index (n) of HSNs aqueous dispersions has a linear relationship with the HSNs volume fraction (V%) in water (Fig. 3d), which follows equation (1).[16, 26]

$$n_t = n_1 V\% + n_2 (1 - V\%) = (n_1 - n_2) V\% + n_2 \quad (1)$$

Where n_t, n_1 and n_2 are refractive index of HSNs aqueous dispersion, HSNs and H_2O. V% is volume fraction of HSNs. As described in Fig. 3d, n_2 is about 1.333 and the slope of the line is 0.009. The function of n_t and V% is fitted linearly (R^2=0.999), namely n_t=0.009V%+1.333. So the refractive index of HSNs (n_1) is the sum of 1.333 and 0.009, namely 1.342. Moreover, the refractive index of HSNs also can be calculated from their size, following the equation (1) too, butn_t, n_1 and n_2 are refractive index of HSNs, solid SiO_2 and air. As we know n_1 and n_2 are about 1.46 and 1 respectively. The shell of HSNs has high porosity. According to the literatures, [27, 28] pore volume of the amorphous SiO_2 is generally about 0.12 cm^3/g. And the ratio of pore volume of the HSNs shell to the whole volume of HSNs can be calculated at 17%, based on the specific volume of 0.73cm^3/g (density of 1.37 g/cm^3) for HSNs. Considering inner cavity volume fraction of 7 %, the total porosity of HSNs is about 24% and theoretical refractive index is 1.350, which shows the theoretical calculation result is in good agreement with experimental one. This also indicates that cavity of HSNs is fully filled with air instead of water. Otherwise, the theoretical and measured value of refractive index for HSNs should be 1.430. In addition, it is satisfactory that the modified HSNs in water are endowed with excellent dispersion stability, still retaining transparent without settlement after placed at half month, due to strong charge repulsion effect among HSNs (-19.2 mv).

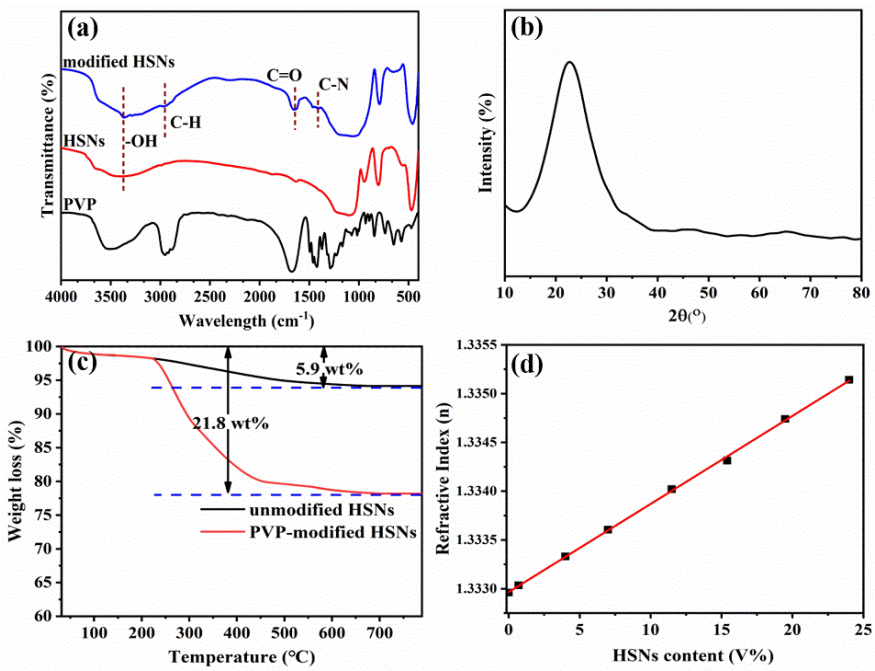

Fig. 3. (a) FT-IR spectra of HSNs. (b) XRD patterns of HSNs. (c) TGA curves of HSNs. (d) The refractive index of aqueous HSNs dispersion.

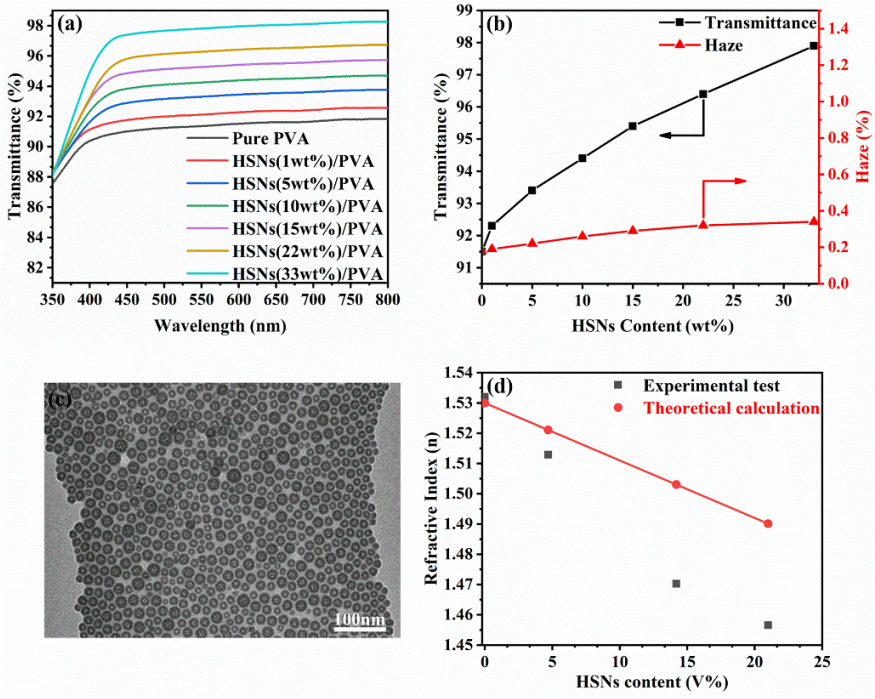

The pure PVA and HSNs/PVA nanocomposites with 10 wt% HSNs have been successfully prepared by the solution blending method and they have the similar transparency in the visible region (Fig. S4, Supporting Information). UV-vis transmittance spectra (Fig. 4a) present optic

Fig. 4 (a) UV-visible transmittance spectra with and without HSNs (b) Transmittance and haze of HSNs/PVA nanocomposites at 580 nm. (c) TEM image of HSNs/PVA nanocomposites with 22 wt% HSNs. (d) Refractive index of HSNs/PVA nanocomposites at 580 nm.

performance of neat PVA and HSNs/PVA nanocomposites. The transmittance of visible light is increased remarkably with the increase in HSNs content, which illustrates that HSNs indeed have an excellent antireflection effect on the nanocomposite films. The visible light transmittance and haze of them at 580 nm are clearly presented in Fig. 4b. When HSNs content increases from 0 to 33 wt%, the visible light transmittance increases from 91.5% to 97.9%, because that the well-dispersed HSNs can decrease surface reflectivity and boost total luminous flux of nanocomposites due to their low refractive index. However, as we know, the existence of nanoparticles in polymer matrix can change the optical path more or less and cause the light diffuse scattering, leading to the increase in reflectivity on the contrary. Although the total reflectivity of nanocomposites may be declined and anti-reflection effect may be realized, the haze of nanocomposite must be increased remarkably, which is a huge obstacle for the application of antireflection transparent composite films.[9, 16] When the particles size is bigger and particles aggregation is more, the haze of composites is raised more obviously. To our surprise, the haze of prepared HSNs/PVA nanocomposite is increased slightly with the addition of HSNs, indicating the excellent dispersion state of HSNs in PVA matrix. As shown in Fig. 4c, HSNs with 22 wt% content have a homogeneous dispersion in PVA matrix without any aggregation. Light diffuse scattering (Rayleigh scattering) does not happen because the particles have the size of much less than 40 nm and are monodispersed in optical polymer matrix basically. [16] In this way, it gives full play to the function of anti-reflection and remarkably improves optical performance of nanocomposites without diffuse reflection. Moreover, HSNs can reduces refractive index of organic matrix obviously (Fig. 4d). It is decreased nonlinearly from 1.535 to 1.458 with increased HSNs volume content from 0 to 21%, which is not consistent with the theoretical calculation results,[26]because the addition of inorganic nanoparticles would reduce the crystallinity of the organic substrate.[29] All these indicate that the HSNs/PVA composite materials have outstanding optical performance with considerable application prospect. Of course, by changing the types of modifiers, the HSNs can be incorporated into the different organic substrates to form nanocomposites with excellent optical properties, which has the widespread application prospect in many different domains.

Conclusion

In this experiment, the sub-20 nm HSNs with the inner cavity diameter of 8 nm can be scaled up in RPB, and they show uniform particles size and excellent monodispersity. As the anti-reflection additive agent, they can be incorporated into optical polymer matrices to reduce the refractive index and improved transparency of polymer effectively. Most importantly, the haze of polymer is unchanged basically by adding HSNs, indicating that HSNs with ultrafine grain size are well-dispersed in polymer matrix. All in all, this work provides a simple and effective method to stably synthesize the ultrafine HSNs, which can promote the development of the technology for the large-scale preparation and industrial application of anti-reflection materials.

Acknowledgement

This work was financially supported by National Natural Science Foundation of China 21776016.

Literature Cited

1. Ma TY, Yu XN, Li HY, et al. High volumetric capacity of hollow structured SnO_2@Si nanospheres for lithium-ion batteries. *Nano Lett.* 2017**;** 17:3959-3964.

2. Lou XW, Archer LA, Yang Z. Hollow micro-/nanostructures: synthesis and applications. *Adv. Mater.* 2008**;** 20:3987-4019.

3. Li BW, Zeng HC. Architecture and preparation of hollow catalytic devices. *Adv. Mater.* 2019**;** 31:1801104.

4. Wang X, Feng J, Bai Y, Zhang Q, Yin Y. Synthesis, properties, and applications of hollow micro-/nanostructures. *Chem. Rev.*2016**;** 116:10983-11060.

5. Yu L, Yu XY, Lou XW. The design and synthesis of hollow micro-/nanostructures: present and future trends. *Adv. Mater.*2018**;** 30:1800939.

6. Dai JY, Zou HB, Shi ZQ, et al. Janus n-doped carbon@silica hollow spheres as multifunctional amphiphilic nanoreactors for base-free aerobic oxidation of alcohols in water. *ACS Appl. Mater. Interfaces.* 2018**;** 10:33474-33483.

7. Chang FP, Hung Y, Chang JH, Lin CH, Mou CY. Enzyme encapsulated hollow silica nanospheres for intracellular biocatalysis. *ACS Appl. Mater. Interfaces.* 2014**;** 6:6883-6890.

8. Zhang J, Ai L, Lin S, et al. Preparation of humidity, abrasion, and dust resistant antireflection coatings for photovoltaic modules via dual precursor modification and hybridization of hollow silica nanospheres. 2019**;** 192:188-196.

9. Loste J, Lopez-Cuesta JM, Billon L, Garay H, Save M. Transparent polymer nanocomposites: An overview on their synthesis and advanced properties. *Prog. Polym. Sci.* 2019**;** 89:133-158.

10. Suthabanditpong W, Takai C, Fuji M, Buntem R, Shirai T. Improved optical properties of silica/UV-cured polymer composite films made of hollow silica nanoparticles with a hierarchical structure for light diffuser film applications. *Phys. Chem. Chem. Phys.*2016**;** 18:16293-16301.

11. Ernawati L, Ogi T, Balgis R, et al. Hollow silica as an optically transparent and thermally insulating polymer additive. *Langmuir.*2016**;** 32:338-345.

12. Hu J, Chen M, Fang XS, Wu LW. Fabrication and application of inorganic hollow spheres. *Chem. Soc. Rev.*2011**;** 40:5472-5491.

13. Wang JY, Cui Y, Wang D. Design of hollow nanostructures for energy storage, conversion and production. *Adv. Mater.*2019**;** 31:24.

14. Prieto G, Tuysuz H, Duyckaerts N, et al. Hollow nano- and microstructures as catalysts. *Chem. Rev.*2016**;** 116:14056-14119.

15. Jia GY, Ji ZH, Wang HN, Chen RY. Preparation and properties of five-layer graded-refractive-index antireflection coating nanostructured by solid and hollow silica particles. *Thin Solid Films.*2017**;** 642:174-181.

16. Althues H, Henle J, Kaskel S. Functional inorganic nanofillers for transparent polymers. *Chem. Soc. Rev.* 2007**;** 36:1454-1465.

17. Hribalova S, Pabst W. Light scattering and extinction in polydisperse systems. *J. Eur. Ceram. Soc.*2020**;** 40:867-880.

18. Cui CW, Yang C, Bao J, et al. Monodispersed ZnO nanoparticle-poly(methyl methacrylate) composites with visible transparency for ultraviolet shielding applications. *ACS Appl. Nano Mater.* 2020**;** 3:9026-9034.

19. Huang XJ, Zeng XF, Wang JX, Zhang LL, Chen JF. Synthesis of monodispersed ZnO@SiO_2 nanoparticles for anti-UV aging application in highly transparent polymer-based nanocomposites. *J. Mater. Sci.* 2019**;** 54:8581-8590.

20. Shi H, He Y, Pan Y, et al. A modified mussel-inspired method to fabricate TiO_2 decorated superhydrophilic PVDF membrane for oil/water separation. *J. Membr. Sci.* 2016**;** 506:60-70.

21. Gao T, Jelle BP, Sandberg LIC, Gustavsen A. Monodisperse Hollow Silica Nanospheres for Nano Insulation Materials: Synthesis, Characterization, and Life Cycle Assessment. *ACS Appl. Mater. Interfaces.* 2013**;** 5:761-767.

22. Kang H, Long DJ, Haynes CL. Preparation of colloidally stable positively charged hollow silica nanoparticles: effect of minimizing hydrolysis on zeta potentials. *Langmuir.*2019**;** 35:7985-7994.

23. Sosso GC, Chen J, Cox SJ, et al. Cystal nucleation in liquids: open questions and future challenges in molecular dynamics simulations. *Chem. Rev.* 2016**;** 116:7078-7116.

24. Wenzel D, Gorak A. Review and analysis of micromixing in rotating packed beds. *Chem. Eng. J.* 2018**;** 345:492-506.

25. Liu HT, Hu TT, Wang D, et al. Preparation of fluorescent waterborne polyurethane nanodispersion by high-gravity miniemulsion polymerization for multifunctional applications. *Chemical Engineering and Processing-Process Intensification.* 2019**;** 136:36-43.

26. Xia Y, Zhang C, Wang JX, et al. Synthesis of Transparent Aqueous ZrO2 Nanodispersion with a Controllable Crystalline Phase without Modification for a High-Refractive-Index Nanocomposite Film. *Langmuir.* 2018**;** 34:6806-6813.

27. Kong L, Uedono A, Smith SV, et al. Synthesis of silica nanoparticles using oil-in-water emulsion and the porosity analysis. 2012**;** 64:309-314.

28. Raschpichler C, Goroncy C, Langer B, Antonsson E, Ruehl EJTJoPCC. Surface Properties and Porosity of Silica Particles Studied by Wide-Angle Soft X-Ray Scattering. 2020**;** XXXX.

29. Karthikeyan B, Hariharan S, Sasidharan A, et al. Optical, vibrational and fluorescence recombination pathway properties of nano SiO2-PVA composite films. *Optical Materials.*2019**;** 90:139-144.